



## Preparation of gradient wettability surface by anodization depositing copper hydroxide on copper surface

Jiang CHENG, Yi-fei SUN, An ZHAO, Zi-heng HUANG, Shou-ping XU

School of Chemistry and Chemical Engineering, South China University of Technology, Guangzhou 510640, China

Received 17 September 2014; accepted 30 December 2014

**Abstract:** A facile route for preparation of gradient wettability surface on copper substrate with contact angle changing from  $90.3^\circ$  to  $4.2^\circ$  was developed. The  $\text{Cu}(\text{OH})_2$  nanoribbon arrays were electrochemically deposited on copper foil via a modified anodization technology, and the growth degree and density of the  $\text{Cu}(\text{OH})_2$  arrays may be controlled varying with position along the substrate by slowly adding aqueous solution of KOH into the two-electrode cell of an anodization system to form the gradient surface. The prepared surface was water resistant and thermal stable, which could keep its gradient wetting property after being immersed in water bath at  $100^\circ\text{C}$  for 10 h. The results of scanning electron microscopy (SEM), X-ray diffraction (XRD) and X-ray photoelectron spectroscopy (XPS) demonstrate that the distribution of  $\text{Cu}(\text{OH})_2$  nanoribbon arrays on copper surface are responsible for the gradient wettability.

**Key words:** gradient wettability surface;  $\text{Cu}(\text{OH})_2$  nanoribbon array; anodization depositing; contact angle

### 1 Introduction

Gradient wettability surfaces have attracted extensive attention in past decades for their potential application in a wide variety of fields, such as microfluidics [1], protein absorption or cell adhesion [2,3], moisture collection [4] and heat transfer enhancement in heating/cooling systems [5,6]. Various techniques for fabricating gradient wettability surfaces including formation of chemical composition gradient (e.g., chemical vapor deposition [7,8], self-assembly [9–11], ionic exchange [12], illumination [13]) and surface roughness gradient (e.g., polymer melting [14], ionic polymerization [15], laser-etching method [16]) have been developed in recent years. The most reported substrates for the gradient generation are related to the silicon or some given expensive materials such as golden surface [10], resulting in limited industrial applications on a large scale. As a kind of important engineering materials, copper has recently generated much interest in surface wettability modification especially in construction of gradient wettability surfaces for the area of heat transfer enhancement, including vapor

condensers for power plants and heat pipes for microelectronic cooling [17–19]. HUANG et al [17] reported a procedure of making wettability gradients on copper, with water contact angles gradually changing from  $88^\circ$  to  $18^\circ$ , by synthesis of cone-like  $\text{Cu}_2\text{O}$  nanostructures using temperature-controlled surface oxidation method. The prepared wettability gradients can enhance the drop-wise condensation rate up to 30%. In the micro-heat pipe system for microelectronic cooling, the wettability gradients inside the inner surface of grooved copper heat pipes were found to be capable of removing a greater amount of heat than the untreated pipes under the same condition [19,20], which may be attributed to the improvement of capillary performance for the back-flow of working liquid from the condensing section to evaporative section. More recently, HUANG and LEU [21] proposed a procedure for precisely fabricating high wettability gradient copper surface using photolithography, hydrogen dioxide immersion and fluorination with Teflon, and droplets on the gradient will exhibit the ability of self-motion from the superhydrophobic to superhydrophilic side.

On the other hand, it is well known that electrochemical procedures can be accurately controlled

and easily magnified on the large scale in industry [22,23]. Up to now, to the best of our knowledge, the fabrication of gradient wettability surface on metal substrates through electrochemical approach has not yet been reported in literatures, even though electrochemical technique has been employed to fabricate uniform superhydrophobic surfaces on copper substrate [22] or water-repellent coatings on gray cast iron surface [24]. Furthermore, there are few publications concerning the water-resistant performance and thermal stability of the gradient wettability surfaces, which are the key factors considered in the heat transfer system with phase change.

In this work, we reported a facile electrochemical approach to prepare a gradient wettability surface on copper substrate. The gradient wettability surface was achieved by varying anodization degree of the copper foil in an aqueous solution of KOH to control the  $\text{Cu}(\text{OH})_2$  nanoribbon arrays electrochemically grown along the copper substrate. The water-resistant property and thermal stability of the gradient surface were tested for potential applications in the heat transfer area.

## 2 Experimental

### 2.1 Fabrication of gradient wettability surface

The copper substrate with dimensions of 50 mm × 10 mm × 0.1 mm (Kermel Chemical Reagent Co., Ltd., Tianjin, China; purity 99.8%) was cleaned successively with acetone, ethanol and a 2.0 mol/L HCl aqueous solution for 5 min each under ultrasonication to remove the grease and get rid of the copper oxides on the surface, and further dried with a dry nitrogen stream before experiment. The growth of  $\text{Cu}(\text{OH})_2$  nanoribbon arrays was carried out in an anodization system under certain applied voltage at room temperature by using a two-electrode cell with copper foil as the working electrode and graphite plate (50 mm × 10 mm × 1.0 mm) as the counter electrode. As shown in Fig. 1, both electrodes were put into a beaker with their terminal standing vertically on the bottom of beaker. Then, a relatively dilute KOH aqueous solution was added slowly into the beaker under a constant current intensity, and the upper surface level of the solution increased gradually as time elapsed. At the same time, the addition speed was tuned to make sure that it would take certain time for the surface of the solution to reach the upper edge of the substrate. After the surface of the solution reached the designed height or the upper end of the substrate, the copper substrate was taken out from the solution, fully rinsed with deionized water, and dried in nitrogen stream. Thus, positions along the latitude of the copper substrate would correspond directly to a continuously changing immersion time or anodization degree (i.e., the anodization degree decreased gradually

from the lower part to upper part along the substrate, which means that different positions of the substrate will possess different growth rates of  $\text{Cu}(\text{OH})_2$  nanoribbon arrays and wettability).

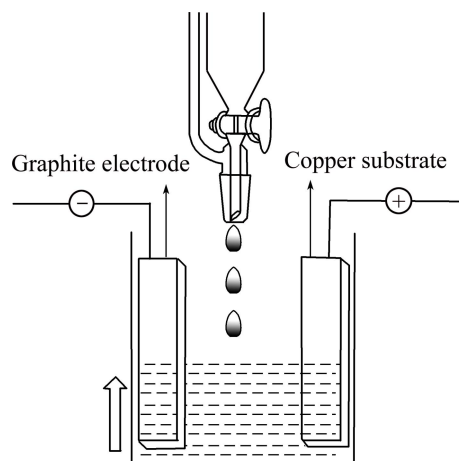


Fig. 1 Scheme of preparation of gradient wettability surface on copper substrate

### 2.2 Characterization

The water contact angles on copper substrate were measured by a contact angle system, OCA15 (Data Physics Instruments Company, Germany) at room temperature. The volume of the individual water droplet used for the static contact angle measurements was 3  $\mu\text{L}$ . The contact angle was obtained by averaging five measurement results at the same position on the gradient wettability surface. Scanning electron microscope (SEM, LEO 1530 VP, Germany) was employed to observe the morphologies of the as-prepared copper substrate and  $\text{Cu}(\text{OH})_2$  nanoribbon arrays. X-ray diffraction (XRD, Bruker, D8 Advance, Germany) was employed to determine the crystallographic structures of  $\text{Cu}(\text{OH})_2$  nanoribbon arrays. Axis ultra X-ray photoelectron spectroscopy (XPS, Vario EL III, Elementary, Germany) equipped with a standard monochromator Al  $K_{\alpha}$  source ( $h\nu=1486.6$  eV) was employed to analyze the chemical compositions and states of the  $\text{Cu}(\text{OH})_2$  nanoribbon array film on copper substrate. The binding energy data were calibrated with respect to the Cu 2p signal of copper substrate at 932.4 eV, and the Cu 2p signal of  $\text{Cu}(\text{OH})_2$  at 933.5 eV.

## 3 Result and discussion

### 3.1 Effect of current density

Figure 2 gives the evolution of water contact angle on the copper substrate with anodization time at different constant current densities.

As shown in Fig. 2, the copper substrate immersed in 3 mol/L KOH aqueous solution at different constant current densities displays diverse wettability. The

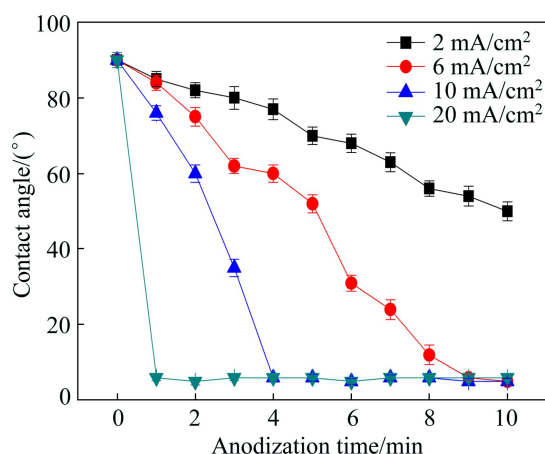
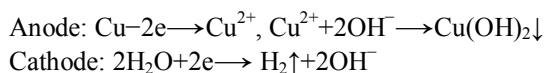


**Fig. 2** Contact angle evolution of copper substrate immersed in 3 mol/L KOH aqueous solution at different current densities

formation of  $\text{Cu}(\text{OH})_2$  arrays is an electrochemical process and can be simply represented by the following two electrochemical half reactions:



In the presence of polar  $-\text{OH}$  groups, the  $\text{Cu}(\text{OH})_2$  nanoribbon array film on copper substrate would show hydrophilic property. When the as-prepared copper substrate is immersed in 3 mol/L KOH aqueous solution at a constant current density of 20  $\text{mA}/\text{cm}^2$ , it takes only 1 min to reach superhydrophilicity with a contact angle lower than  $5^\circ$ . Further anodization of the substrate in solution may result in a very little decrease of the water contact angle of copper surface, which suggests that in such a short time the  $\text{Cu}(\text{OH})_2$  nanoribbon arrays have electrochemically grown to form complete hydrophilic film. By adjusting the constant current density, different wettability properties with anodization time can be obtained. Low current density will lead to obviously decreased growth rate of  $\text{Cu}(\text{OH})_2$  nanoribbon arrays on copper substrate. When the constant current density is set at 6  $\text{mA}/\text{cm}^2$ , it would take nearly 9 min for  $\text{Cu}(\text{OH})_2$  nanoribbon arrays to gradually form a superhydrophilic film on copper substrate. Thus, 6  $\text{mA}/\text{cm}^2$  may be taken as the typically acceptable current density for construction of the gradient wettability surface, because it provides relatively proper and stable reaction dynamics and facilitates the realization of a gradient wettability surface on copper substrate from the original contact angle of copper substrate to superhydrophilic.

### 3.2 Effect of concentration of KOH solution

Figure 3 demonstrates the evolution of water contact angle on the copper substrate with anodization time at a constant current density of 6  $\text{mA}/\text{cm}^2$  in different concentrations of KOH aqueous solution.

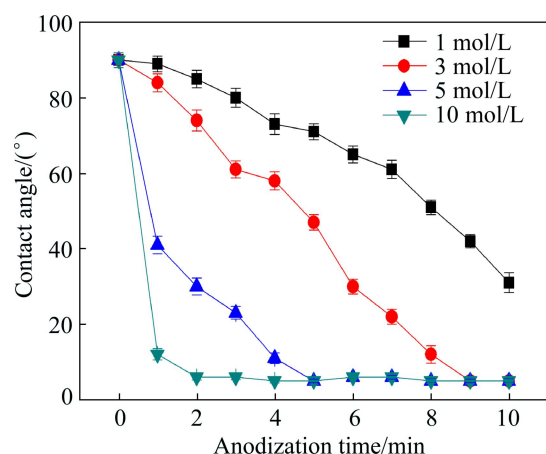


**Fig. 3** Contact angle evolution of copper substrate immersed in different concentrations of KOH aqueous solution at current density of 6  $\text{mA}/\text{cm}^2$

As can be seen from Fig. 3, it takes only 2 min to reach superhydrophilicity with a contact angle lower than  $5^\circ$  when the copper substrate is immersed in 10 mol/L KOH aqueous solution at a constant current density of 6  $\text{mA}/\text{cm}^2$ . Lower concentration of KOH aqueous solution will decrease the growth of  $\text{Cu}(\text{OH})_2$  nanoribbon arrays electrochemically on the copper substrate and in turn slow down the changing rate of contact angle. When the copper substrate is immersed in 3 mol/L KOH aqueous solution at current density of 6  $\text{mA}/\text{cm}^2$ , it would take nearly 9 min for  $\text{Cu}(\text{OH})_2$  nanoribbon arrays to gradually form a superhydrophilic film on the copper substrate. Similarly, a KOH aqueous solution concentration of 3 mol/L is taken as the suitable concentration to make the fabricating process controllable and satisfy the requirement of precise design for the gradient wettability surface.

### 3.3 Contact angle analysis

As described in the experimental section, the as-prepared copper substrate was used as the working electrode and graphite as the counter electrode, and both were put in a beaker with their terminal standing vertically on the bottom of the beaker. The constant current density was kept at 6  $\text{mA}/\text{cm}^2$ , and the 3 mol/L KOH aqueous solution was then added slowly into the beaker. Positions along the latitude of the substrate would correspond directly to a continuously changing growth rate of  $\text{Cu}(\text{OH})_2$  nanoribbon arrays and a certain wettability. As predicted, the prepared substrate did exhibit a gradient wetting property. As shown in Fig. 4, the contact angles change continuously along the surface from  $90.3^\circ$  to  $4.2^\circ$  in about 2 cm length of the copper substrate, indicating that a gradient wettability surface from the original contact angle of copper to superhydrophilic state is prepared.



**Fig. 4** Photograph of water contact angle along gradient surface (The photograph is combined with three continuous photographs along the length of copper substrate because the view angle of the contact angle measurement system is not wide enough. The volume of the water droplets is kept at about 3  $\mu\text{L}$ )

The copper substrate was kept in a hot water bath at round 100  $^{\circ}\text{C}$  for 10 h to test the water resistant property and thermal stability of the prepared gradient wettability surface. A comparison between the contact angles of different positions on copper substrate before and after immersion in hot water as shown in Fig. 5 demonstrates that only little change in contact angle occurs along the length of the copper substrate surface, which could be anticipated for the prepared gradient wettability surface to be applied in the industry environment of high-temperature or high-moisture such as heat transfer with phase change.

### 3.4 Morphology observation

Figure 6 shows the SEM images of different positions surface along the copper substrate. The wettability varies with the growth condition of  $\text{Cu}(\text{OH})_2$  nanoribbon arrays along the latitude of the substrate.

From Fig. 6(a), there is not any  $\text{Cu}(\text{OH})_2$  nanoribbon array at all for the original copper substrate

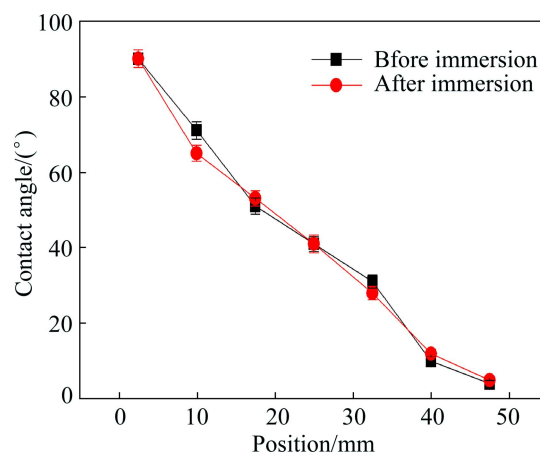


**Fig. 5** Comparison of contact angles before and after immersion in water bath at 100  $^{\circ}\text{C}$  for 10 h

with its contact angle of 90.3 $^{\circ}$ . In Fig. 6(b), some  $\text{Cu}(\text{OH})_2$  nanoribbon arrays with relatively short length and low growth density can be observed when the contact angle is 52.7 $^{\circ}$ . Compared with Fig. 6(b), the  $\text{Cu}(\text{OH})_2$  nanoribbon arrays in Fig. 6(c) corresponding to a contact angle of 27.3 $^{\circ}$  possess greater growth density. In Fig. 6(d), the density of  $\text{Cu}(\text{OH})_2$  nanoribbon arrays increases abruptly due to the change of surface nanostructure from nanoribbons to bundles of nanowires and the superhydrophilic copper surface with contact angle of 4.2 $^{\circ}$  is achieved. The above results demonstrate that the density and length of  $\text{Cu}(\text{OH})_2$  nanoribbon arrays increase little by little with immersion time (reaction

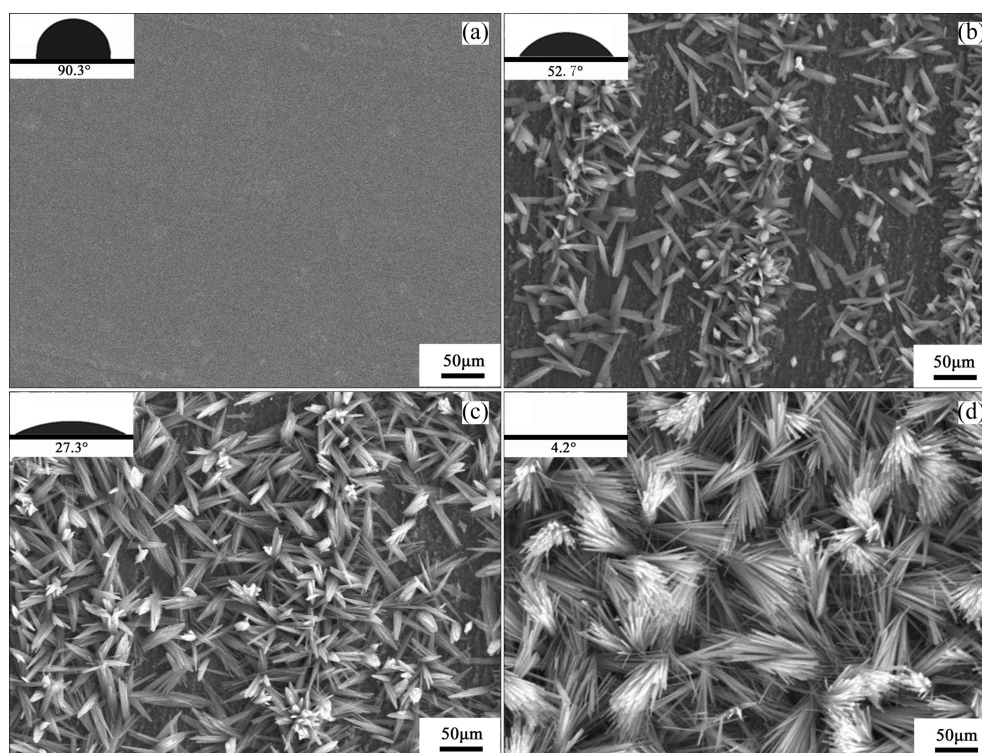


**Fig. 6** SEM images of  $\text{Cu}(\text{OH})_2$  nanoribbon arrays growth on copper substrate

time), leading to the contact angle of copper surface decreasing gradually. Therefore, the gradient wettability of copper substrate is closely related to the  $\text{Cu}(\text{OH})_2$  nanoribbon arrays electrochemically grown on the substrate.

By further comparing the SEM images between Fig. 6(c) (before immersion in hot water) and Fig. 7 (after immersion) corresponding to the point on copper substrate with a contact angle of around  $27.7^\circ$ , no significant difference could be found in surface morphologies of  $\text{Cu}(\text{OH})_2$  nanoribbon arrays, which also indicates the water resistance and thermal stability of the prepared gradient surface as described above.

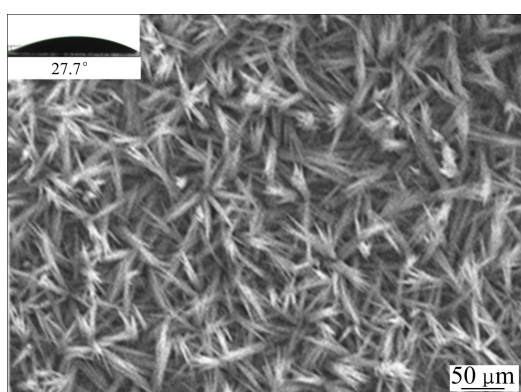


**Fig. 7** SEM image of  $\text{Cu}(\text{OH})_2$  nanoribbon arrays on copper surface at point with contact angle of  $27.7^\circ$  after immersion in  $100^\circ\text{C}$  water bath for 10 h

### 3.5 Composition analysis

The crystal structure of the  $\text{Cu}(\text{OH})_2$  nanoribbon arrays on copper substrate (Fig. 8) was determined by X-ray diffraction (XRD) analysis. Figures 8(a) and (b) represent the two points of the  $\text{Cu}(\text{OH})_2$  nanoribbon arrays on the substrate, whose contact angles are  $90.3^\circ$  and  $4.2^\circ$ , respectively. As shown in Fig. 8(a), all the peaks marked with asterisk can be readily indexed to orthorhombic-phase Cu (JCPDS card No.85–1326). In Fig. 8(b), all of the XRD peaks marked with black dot can be indexed to orthorhombic-phase  $\text{Cu}(\text{OH})_2$  (JCPDS card No. 72–0140) except those marked with asterisk of the copper substrate (JCPDS card No. 85–1326).

Furthermore, we made spatially resolved X-ray photoelectron spectroscopy (XPS) measurements to provide a semiquantitative analysis, which could help to confirm a surface chemical composition gradient depending on the control of  $\text{Cu}(\text{OH})_2$  nanoribbon array growth along the copper substrate. As shown in Fig. 9, the peak at 932.4 eV is related to the Cu 2p signal of copper substrate, and that at 933.5 eV is associated with the Cu 2p signal of  $\text{Cu}(\text{OH})_2$ . The Cu 2p peak of  $\text{Cu}(\text{OH})_2$  enhances from Figs. 6(a) to (c) while the contact angles of three points decrease gradually.

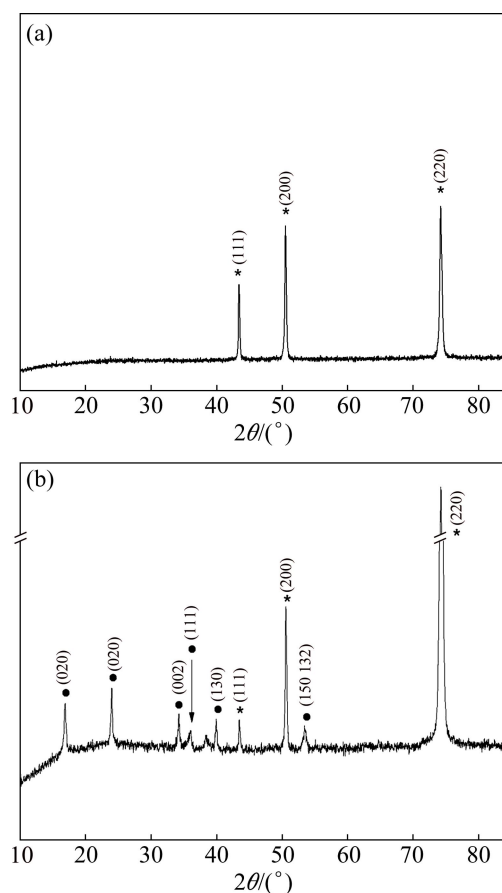


**Fig. 8** XRD patterns of  $\text{Cu}(\text{OH})_2$  nanoribbon arrays on copper substrate with different contact angles of  $90.3^\circ$  (a) and  $4.2^\circ$  (b)

The peak area of XPS Cu 2p core level spectra may be used to roughly explain the principle of wettability gradient formation on the copper substrate. As shown in Table 1, the peak area of  $\text{Cu}(\text{OH})_2$  increases with immersion time due to an increase of the amount of  $\text{Cu}(\text{OH})_2$  formed on copper surface as the  $\text{Cu}(\text{OH})_2$  nanoribbon arrays grow gradually. The ratio of  $S_{\text{Cu}}/S_{\text{Cu}(\text{OH})_2}$  in Table 1 decreases from Figs. 6(a) to (c), implicating that the density of  $\text{Cu}(\text{OH})_2$  nanoribbon arrays over copper substrate increases gradually, which accounts for the wettability gradient on copper substrate.

## 4 Conclusions

The gradient wettability surface with water contact angle changing from  $90.3^\circ$  (the original contact angle of copper) to  $4.2^\circ$  is successfully prepared by anodization depositing copper hydroxide  $\text{Cu}(\text{OH})_2$  nanoribbon arrays on the copper substrate. It is based on the control of  $\text{Cu}(\text{OH})_2$  nanoribbon arrays electrochemically grown on copper substrate through varying the anodization time corresponding to different positions along the substrate surface in an aqueous solution of KOH. The gradient wettability properties of the copper substrate are

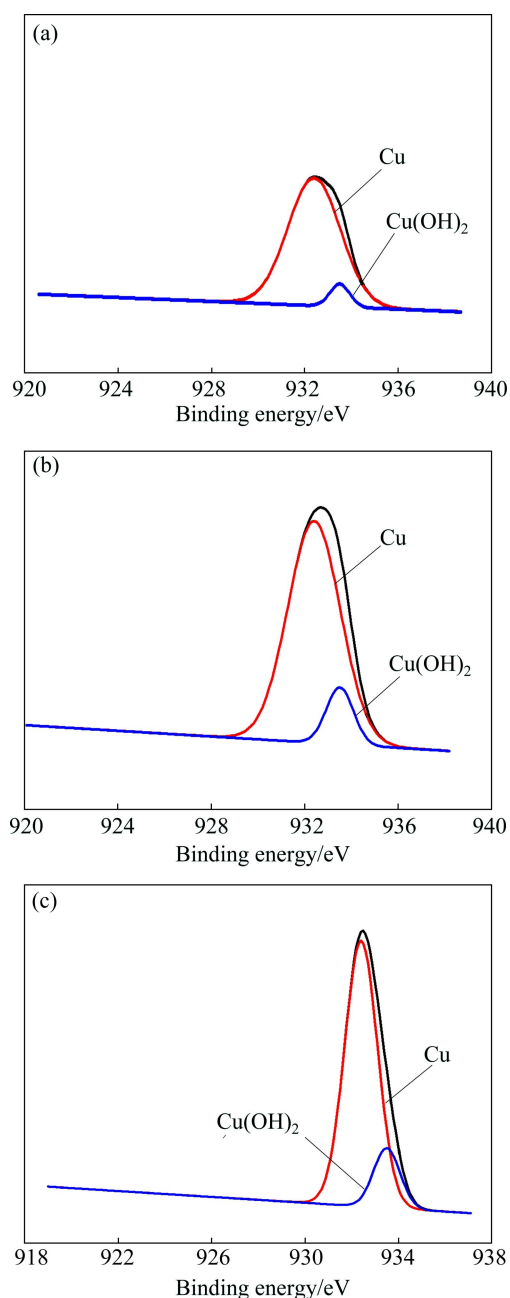


**Fig. 9** High-resolution XPS spectra of Cu(OH)<sub>2</sub> nanoribbon arrays on copper substrate with different contact angles of 90.3° (a), 40.7° (b) and 4.2° (c)

**Table 1** Peak area of XPS Cu 2p core level spectra along copper substrate

Fig. 6	Contact angle/(°)	$S_{\text{Cu}}$	$S_{\text{Cu(OH)}_2}$	$S_{\text{Cu}}/S_{\text{Cu(OH)}_2}$
(a)	90.3	15117	1003	15.07
(b)	40.7	35940	4714	7.62
(c)	4.2	33194	6000	5.53

thermally stable and water-resistant. This work is anticipated to provide a new strategy for preparing gradient wettability surface on copper substrate with potential application in heat transfer systems with phase change.

## References

- [1] ZHU X, WANG H, LIAO Q, DING Y D, GU Y B. Experiments and analysis on self-motion behaviors of liquid droplets on gradient surfaces [J]. *Experimental Thermal and Fluid Science*, 2009, 33(6): 947–954.
- [2] GLASSFORD S, CHAN K L A, BYME B, KAZARIAN S G. Chemical imaging of protein adsorption and crystallization on a wettability gradient surface [J]. *Langmuir*, 2012, 28(6): 3174–3179.
- [3] SHIN Y N, KIM B S, AHN H H, LEE J H, KIM K S, LEE J Y, KIM M S, KHANG G, LEE H B. Adhesion comparison of human bone marrow stem cells on a gradient wettability surface prepared by corona treatment [J]. *Applied Surface Science*, 2008, 255(2): 293–296.
- [4] JU J, XIAO K, YAO X, BAI H, JIANG L. Bioinspired conical copper wire with gradient wettability for continuous and efficient fog collection [J]. *Advanced Materials*, 2013, 25: 5937–5942.
- [5] DANIEL S, CHAUDHURY M K, CHEN J C. Fast drop movements resulting from the phase change on a gradient surface [J]. *Science* 2001, 291: 633–636.
- [6] LIAO Q, GU Y B, ZHU X, WANG H, XIN M D. Experimental investigation of dropwise condensation heat transfer on the surface with a surface energy gradient [J]. *Journal of Enhanced Heat Transfer*, 2007, 14(3): 243–256.
- [7] CHAUDHURY M K, WHITESIDES G M. How to make water run uphill [J]. *Science*, 1992, 256(5063): 1539–1541.
- [8] HANDESRIS B, SOUPREMANIEN U, DUNOYER N. Uphill motion of droplets on tilted and vertical grooved substrates induced by a wettability gradient [J]. *Colloids and Surfaces A: Physicochemical and Engineering Aspects*, 2013, 434: 126–135.
- [9] MEYYAPPAN S, SHADNAM M R, AMIRFAZLI A. Fabrication of surface energy/chemical gradients using self-assembled monolayer surfaces [J]. *Langmuir*, 2008, 24(6): 2892–2899.
- [10] YU X, WANG Z Q, JIANG Y G, ZHANG X. Surface gradient material: From superhydrophobicity to superhydrophilicity [J]. *Langmuir*, 2006, 22(10): 4483–4486.
- [11] HU B H, XUE L J, YANG P, HAN Y C. Variable-focus liquid microlenses with adjustable 3-D curved housings [J]. *Langmuir*, 2010, 26(9): 6350–6356.
- [12] WANG L M, PENG B, SU Z H. Tunable wettability and rewritable wettability gradient from superhydrophilicity to superhydrophobicity [J]. *Langmuir*, 2010, 26(14): 12203–12208.
- [13] ITO Y, HEYDARI M, HASHIMOTO A, KONNO T, HIRASAWA A, HORI S, KURITA K, NAKAJIMA A. The movement of a water droplet on a gradient surface prepared by photodegradation [J]. *Langmuir*, 2007, 23(4): 1845–1850.
- [14] ZHANG J L, XUE L J, HAN Y C. Fabrication gradient surfaces by changing polystyrene microsphere topography [J]. *Langmuir*, 2005, 21(1): 5–8.
- [15] LI X F, DAI H J, TAN S X, ZHANG X Y, LIU H Y, WANG Y X, ZHAO N, XU J. Facile preparation of poly (ethyl  $\alpha$ -cyanoacrylate) superhydrophobic and gradient wetting surfaces [J]. *Journal of Colloid and Interface Science*, 2009, 340(1): 93–97.
- [16] SUN C, ZHAO X W, HAN Y H, GU Z Z. Control of water droplet motion by alteration of roughness gradient on silicon wafer by laser surface treatment [J]. *Thin Solid Films*, 2008, 516(12): 4059–4063.
- [17] HUANG Z, LU Y X, QIN H S, YANG B, HU X J. Rapid Synthesis of wettability gradient on copper for improved drop-wise condensation [J]. *Advanced Engineering Materials*, 2012, 14(7): 491–496.
- [18] ZHANG Y, PI P H, WEN X F, ZHENG D F, CAI Z Q, CHENG J. Construction and application of wettability gradient surfaces [J]. *Progress in Chemistry*, 2011, 23(12): 2457–2461.

- [19] HU Y X, CHENG J, ZHANG W, SHIRAKASHI R, WANG S F. Thermal performance enhancement of grooved heat pipes with inner surface treatment [J]. International Journal of Heat and Mass Transfer, 2013, 67: 416–419.
- [20] QU J, WU H Y, CHENG P. Effects of functional surface on performance of a micro heat pipe [J]. International Communications in Heat and Mass Transfer, 2008, 35(5): 523–528.
- [21] HUANG D J, LEU T S. Fabrication of high wettability gradient on copper substrate [J]. Applied Surface Science, 2013, 280: 25–32.
- [22] WU X F, SHI G Q. Production and characterization of stable superhydrophobic surfaces based on copper hydroxide nanoneedles mimicking the legs of water striders [J]. J Phys Chem B, 2006, 110: 11247–11252.
- [23] YAN H, KUROGI K, MAYAMA H, TSUJII K. Environmentally stable super water-repellent poly (alkylpyrrole) films [J]. Angewandte Chemie International Edition, 2005, 44(22): 3453–3456.
- [24] LIU Yan, LI Liang, LU Guo-long, HAN Zhi-yu, LIU Jin-dan, YU Si-rong. Fractal characteristics and wettability of Nano- $\text{Al}_2\text{O}_3/\text{Ni-Co}$  composite coating prepared by electrodeposition [J]. Transactions of Nonferrous Metals Society of China, 2011, 21(S2): s380–s383.

## 阳极氧化沉积氢氧化铜法制备梯度润湿铜表面

程 江, 孙逸飞, 赵 安, 黄子恒, 徐守萍

华南理工大学 化学与化工学院, 广州 510640

**摘 要:** 提出一种在金属铜上制备梯度润湿表面(接触角变化范围  $90.3^\circ\sim 4.2^\circ$ )的简易方法。采用改进的阳极氧化电沉积技术, 通过向阳极氧化系统的双电极容器中滴加氢氧化钾溶液, 使铜箔电极上氢氧化铜纳米带阵列的生长程度与密度随铜箔高度而变化, 从而形成润湿性梯度。所制备的润湿梯度铜表面具有耐热耐水特性, 当此铜表面置于  $100^\circ\text{C}$  的水浴中 10 h 后仍保持其润湿性梯度。SEM、XRD 和 XPS 测试结果表明, 铜表面的氢氧化铜纳米带阵列的生长特性与分布是形成润湿性梯度的主要原因。

**关键词:** 梯度润湿表面; 氢氧化铜纳米带阵列; 阳极氧化电沉积; 接触角

(Edited by Xiang-qun LI)